Detection and Attribution of Thermal Anomalies in Urban Blocks of Qom Using Time-Series Analysis of TIR Imagery

Sajad Sayadi[1]*, Amirali Emamisaleh[2], Alireza Safdarinezhad[2], Alireza Kalaei[2]

[1]Department of Photogrammetry and Remote Sensing, Faculty of Geodesy and Geomatics Engineering, K. N. Toosi University of Technology, Tehran 19967-15433, Iran
[2]Department of Geodesy and Surveying Engineering, Tafresh University, Tafresh, 39518-79611, Iran
* Corresponding Author. Email address: s.sayadi@email.kntu.ac.ir

Keywords: Change Detection, Land Surface Temperature (LST), Time-Series Analysis, Anomaly Detection, Reed-Xiaoli (RX) Algorithm.

Abstract

Rapid urbanization and land-use changes have significantly impacted urban thermal patterns. However, many studies rely on annual or summer-averaged Land Surface Temperature (LST) data, while analysis at the urban block scale, which is crucial for decentralized planning, has received less attention. To address this gap, this research presents an innovative approach to identify thermal anomalies at the urban block level in Qom, Iran, using wintertime Landsat 8 imagery over a ten-year period (2014–2023). The choice of the winter season, due to minimal vegetation cover, allows for a more accurate detection of physical changes and is also favorable for finding the probable energy waste over the city blocks. In this study, time series of outlier-free average and standard deviation values of Land Surface Temperature (LST) were extracted for 499 urban blocks. The probable outlier samples of each city block were found by Median Absolute Deviation (MAD) statistical test. Subsequently, by use of two different versions of the Reed-Xiaoli (RX) algorithm for anomaly detection, blocks with unusual thermal behavior were identified. The results indicated that the 22 identified blocks experienced significantly greater temperature variations (up to 9.07°C) compared to other blocks. Validation of these findings with Google Earth satellite imagery confirmed a direct correlation between the thermal anomalies and actual land-use changes, such as new construction or alterations in land covers. This method proved its effectiveness as a practical tool for monitoring urban developments for supporting decision-making in urban management.

1. Introduction

Urbanization's extremely high rate and highly intensive land-use change dramatically affected regional climate conditions, prompting the creation of thermal anomalies in cities (Ullah et al., 2023). In addition to standard methods for monitoring land-use conversions e.g., multispectral and hyperspectral remote sensing imagery (Fakhri et al., 2022), characterization of the Land Surface Temperature (LST) (Kachar et al., 2015), in particular, with time series for remotely sensed thermal infrared imagery, has turned out to be an extremely useful tool for the characterization of thermal dynamics (Salih et al., 2018).

In this respect, a high percentage of research has explored thermal patterns within cities. For instance, identification of summer as well as winter hot spots within different seasons within the city of Yazd, Iran, was made through the utilization of Landsat 8 imagery in addition to machine learning algorithms by (Mansourmoghaddam et al., 2024). Spatiotemporally replicable LST was presented in their work through the presentation of the appropriateness of employing time-series analysis in conjunction with machine learning for the identification of morphological urban variations (Mansourmoghaddam et al., 2024). In a similar vein, the extraction of long-term Permanent Urban Heat Islands (PUHIs) within Tehran was made through the assistance of Landsat 8 imagery which demonstrated the appropriateness of long-term time-series analysis in LST for thermal anomaly tracking within cities (Kalhor et al., 2024). They recognized that industrial centers, bare earth regions, as well as commercial concentrations, were located northward as well as westward of this metropolitan area as PUHIs.

(Xian et al., 2023) analyzed three decades' LST patterns within the top 50 cities in the United States through simultaneous analyses of land cover maps and LST data. Their findings revealed that different patterns in land cover changes in cities' urban areas bear different features that affect LST patterns in cities, with surprising interaction in thermal dynamics and cities' land-use change (Xian et al., 2023). (Evgrafova et al., 2024) analyzed LST distribution within four mid-scale Siberia and Urals cities within a ten-year period. Building density showed the highest correlation with temperature in cities, where ground elevation, as well as elevation of buildings, tend to yield low impact in thermal distribution confirming morphology as an important cause in change of LST (Evgrafova et al., 2024).

(Edan et al., 2021) also investigated land-use change as well as seasonal LST impact in Al-Kut, Iraq. Results presented a significant area expansion in the cities and reduced vegetation cover, leading to a rise in summer as well as winter LST. It exhibited a positive correlation with LST as well as NDBI, while a negative correlation with NDVI as well as NDWI was exhibited (Edan et al., 2021). (Effat et al., 2014) analyzed three decades' land cover change as well as Cairo urban heat islands using Landsat data. Results exhibited extensive expansion of cities with lower NDVI values, where a rise in LST occurred over deserts (Effat and Hassan, 2014).

(Huang and Wang, 2019) made a step up from conventional 2D landscape indicators with the integration of 2D as well as 3D urban morphology (e.g., sky view factor, building height) in LST analysis. Even though vegetation cover, a 2D variable, dominated, 3D features also significantly contributed towards moderating the urban temperature (Huang and Wang, 2019). (Dutta et al., 2018) analyzed Indian megacity UHIs' spatiotemporal patterns with a time series from Landsat TM as well as OLI/TIRS imagery. In connecting LST variations with uncontrolled urban sprawl as well as vegetation cover substitution with impervious surfaces, their work contributed towards informing future smart city expansion as well as toward developing relevant urban planning strategies (Dutta et al., 2018).

Although there are an increasing number of studies in the literature, most studies are based on year/summer-averaged LST, whereas winter LST data with minimum vegetation coverage can provide a cleaner substrate for non-vegetational change detection. Also, the analysis of LST in urban regions in the cold part of the year could be beneficial in finding the energy waste regions. Additionally, the concurrent utilization of statistical refinement procedures (e.g., MAD) with the RX anomaly detection algorithm is completely nonexistent. Lastly, too many of the existing analyses were conducted based on citywide/regionwide coverage, whereas for decentralized planning and management, analysis at the denser scale of the urban block is very crucial.

Thus, for the present study, Qom is selected with a goal to identify its potentially thermal anomalous city blocks through retrieving wintertime LST and standard deviation (STD) time series for the period between 2014 and 2023 from Landsat 8 imagery. The proposed method is applied to 499 of Qom urban blocks and results are visually cross-checked with Google Earth.

2. Study Area and Dataset

The study area is the city of Qom, Iran, which serves as an appropriate case for investigating thermal anomalies due to its rapid urban development. For this research, 499 urban blocks were manually delineated in Google Earth and used as the blocks of analysis (Figure 1).

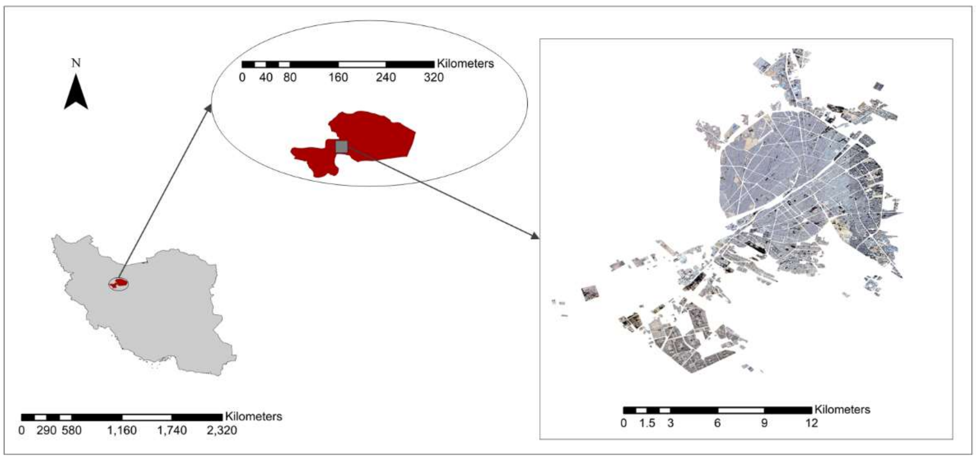

Figure 1. Map of the study area showing the delineated 499 urban blocks in Qom.

The data used in this study includes thermal bands 10 and 11 from Landsat 8 satellite imagery, covering the winter months (December, January, and February) from 2014 to 2023. These months were selected because of the minimal vegetation cover, which facilitates better detection of anomalies associated with land-use changes.

3. Methodology

The methodology is designed to identify statistically significant temporal anomalies in the thermal behavior of urban blocks. As illustrated in Figure 2, the process comprises three main stages.

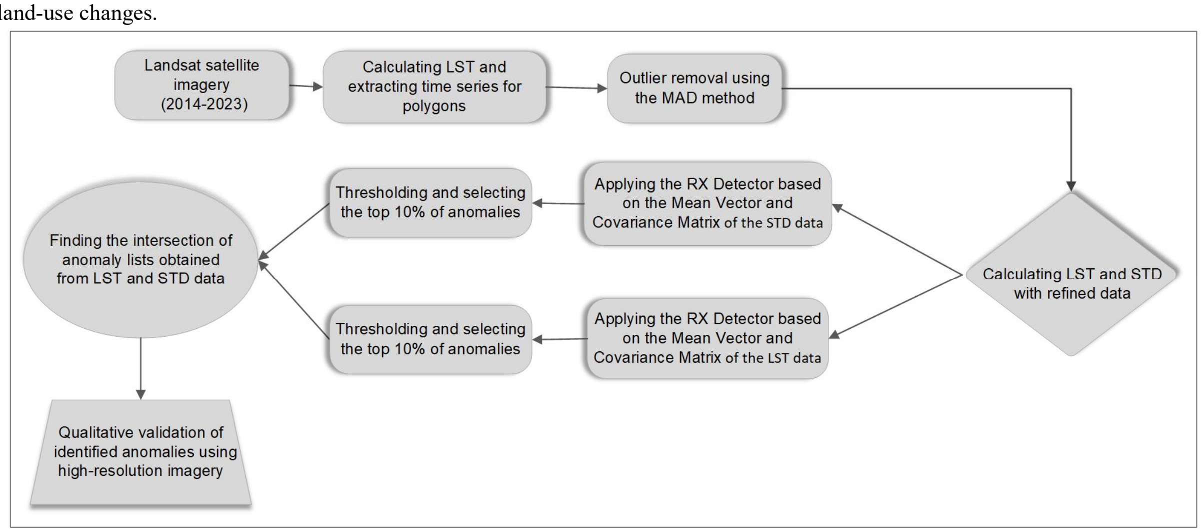

Figure 2. General flowchart of the proposed methodology

This study followed a structured three-phase approach: (1) generation and preprocessing of time-series data, (2) anomaly detection using the Reed-Xiaoli (RX) algorithm, and (3) selection and validation of final candidate blocks representing thermal anomalies. This multi-step framework was designed to reliably identify a subset of urban regions undergoing statistically significant thermal changes. The overall methodology aimed to reduce data noise while maximizing the detection of genuine environmental changes in the urban thermal landscape.

3.1 Time-Series Generation and Preprocessing

As a foundational step, ten-year time series of Land Surface Temperature (LST) data were generated for each of the 499 urban blocks identified within the study area. These time series were constructed using all available cloud-free satellite imagery captured during the study period (2014-2023). To ensure temporal consistency and to reduce the influence of short-term or seasonal fluctuations that are not indicative of long-term land use changes, data extraction was limited to a specific three-month winter window (December through February) for each year.

Focusing on the winter season was critical, as it generally offers more stable atmospheric conditions (based on the typical climatic conditions of Qom) and avoids the thermal distortions caused by extreme summer heat. Furthermore, vegetation cover tends to be at its lowest during winter in the study region, meaning the recorded temperatures are less affected by plant transpiration and more directly reflect changes in land surface composition, which is particularly useful for capturing thermal signals from land use transitions. For each winter season, a representative mean LST and standard deviation (STD) were computed for each block, following the removal of outliers. This process results in 20 (10+10) features for each city block, representing its thermal condition during each winter season. While LST provides a direct measure of thermal magnitude, STD captures thermal variability within a block, offering a complementary perspective on surface heterogeneity and internal urban complexity.

Outlier removal was performed using the Median Absolute Deviation (MAD) method (Zhang et al., 2025), a robust, non-parametric statistical approach. This method was selected for its proven resilience against extreme values and its ability to handle datasets that may deviate from normal distribution or include significant outliers that could distort mean-based techniques. Unlike mean-sensitive methods, MAD calculates deviations relative to the median, making it less susceptible to anomalies. A data point was classified as an outlier if it satisfied Equation (1).

$$\frac{\left| LST_i - LST_{Median} \right|}{MAD} < k \tag{1}$$

where LST_{Median} represents the median value of LST for the given city block at each epoch of data acquisition, and k is a sensitivity threshold, set to 5 empirically in this study. This threshold was deliberately chosen to ensure a conservative but effective removal strategy, targeting only the most aberrant data points, those likely to stem from chimney effects, sensor malfunctions, atmospheric interference, or residual cloud contamination. Importantly, this method preserves genuine LST fluctuations that might reflect actual environmental phenomena. MAD was calculated using Equation (2).

$$\text{MAD} = \text{median}\ (\,|\,\text{LST}_i - \text{LST}_{Median}|) \tag{2}$$

This comprehensive outlier elimination resulted in two refined time series datasets for each block: one for LST and one for STD. These curated datasets served as the input for the next critical phase, which was anomaly detection.

3.2 Anomaly Detection Using Reed-Xiaoli (RX) Algorithm

To detect subtle yet meaningful thermal anomalies within the refined time-series data, the Reed-Xiaoli (RX) algorithm was applied (Zhao et al., 2016). Originally developed for unsupervised anomaly detection in hyperspectral imagery, RX is well-suited for identifying targets that deviate from a statistical background model. In this study, the algorithm was adapted to highlight urban blocks whose temporal thermal behaviour significantly diverged from the broader statistical pattern observed across all blocks over the ten-year period.
The RX process begins by constructing a background statistical model of the entire dataset using two key parameters:

- Mean vector (μ): A 10-dimensional vector (corresponding to the ten study years), where each element represents the average LST (or STD) across all 499 blocks for a specific year. This vector defines a "typical" thermal evolution across the urban area.
- Covariance matrix (Σ): A 10×10 matrix capturing both year-to-year thermal variability and inter-annual correlations within the dataset. This matrix encodes the complex dependencies and temporal dynamics among the urban blocks and ensures that anomaly detection considers not only static deviations but also changes in time-based patterns.

For each block's time series, the Mahalanobis distance from the global mean vector μ was computed. This distance metric effectively accounts for correlations among variables (in this case, annual LST or STD values) and provides a more nuanced measure of deviation than simple Euclidean distance. The resulting Mahalanobis distance serves as the RX anomaly score, defined in Equation (3):

$$\text{RX}\ (x) = (x - \mu)^{T}\ \Sigma^{-1}\ (x - \mu) \tag{3}$$

A higher RX score indicates a greater statistical divergence from the typical urban thermal trend. In practical terms, a block with a high RX score exhibits temporal thermal behavior that is unusual compared to the collective norm, making it a strong anomaly candidate. Unlike simpler methods that flag only extreme temperatures, the RX algorithm excels at highlighting time-series patterns that are contextually out of place.

3.3 Selection and Validation of Final Candidates

After computing RX anomaly scores for all 499 blocks in both the LST and STD analyses, a thresholding step was performed. To focus on the most prominent anomalies, the top 10% of blocks with the highest RX scores were selected from each analysis, resulting in two separate lists of potential anomalies. The final list of high-confidence candidates for land use change was then determined by simply finding the intersection of these two lists, as expressed in Equation (4).

$$\text{Final\_Anomalies} = \text{Anomalies}_{\text{LST}} \cap \text{Anomalies}_{\text{STD}} \tag{4}$$

This process yielded a final list of 22 candidate blocks for further investigation. These blocks were subsequently qualitatively validated using High-Resolution Satellite imagery (HRSI) from Google Earth.

https://doi.org/10.5194/isprs-annals-X-4-W8-2025-693-2026 | © Author(s) 2026. CC BY 4.0 License.

3.4 Identification and Spatial Distribution of Anomalies

A total of 22 urban blocks were identified as final candidates for thermal anomalies. Their spatial distribution across the study area is illustrated in Figure 3.

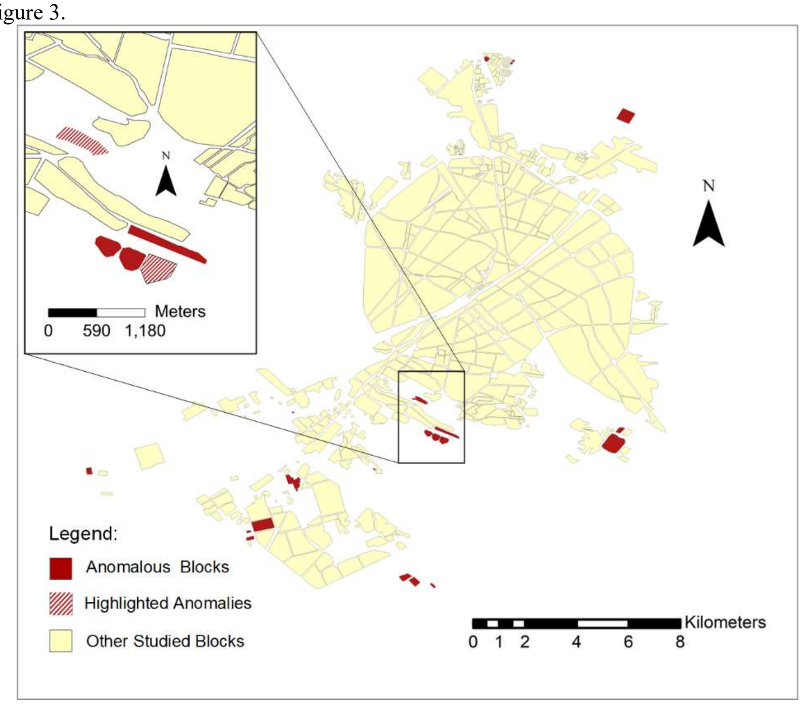

Figure 3. Spatial distribution of anomalous urban blocks. Out of 499 studied blocks, 22 were identified as anomalies (maroon), of which two specific case studies, which will be discussed in the qualitative validation, are highlighted with a hatch pattern.

4. Results

Observing the distribution of recognized anomalies offers a visual insight into areas prone to change and development within the urban context. It is evident that the identified blocks with significant anomalies are predominantly found around the city's periphery. This pattern indicates that the urban fringe of the city exhibits more land-use changes compared to its central regions.

4.1 Quantitative Analysis of Thermal Variations

To gain a clearer understanding of the magnitude and nature of these variations, a more in-depth quantitative analysis was conducted on blocks with the highest and lowest anomaly scores. Table 1 presents the maximum ten-year differences in LST (ΔLST) and thermal standard deviation (ΔSTD) for the five blocks exhibiting the most prominent anomalies (Final Candidates). These values indicate the intensity of thermal fluctuations over the study period and serve as a metric for anomaly magnitude.

ID	Maximum difference in LST(°C)	Maximum difference in STD(°C)
ROI-500	7.26	5.56
ROI-154	6.57	11.00
ROI-98	8.27	12.21
ROI-96	9.07	13.21
ROI-153	6.02	10.35

Table 1. Maximum 10-year difference in LST and STD for the top 5 anomalous urban blocks

Conversely, Table 2 displays the maximum ten-year differences in LST and STD for the five blocks with the lowest anomaly scores (Lowest RX Scores). A close comparison of these two tables reveals significant disparities in the range of thermal variations between blocks identified as anomalous and those exhibiting more stable thermal behaviour.

ID	Maximum difference in LST(°C)	Maximum difference in STD(°C)
ROI-217	4.31	6.10
ROI-358	3.90	4.38
ROI-381	3.10	5.16
ROI-377	3.58	4.73
ROI-311	3.35	4.27

Table 2. Maximum 10-year difference in LST and STD for the bottom 5 anomalous blocks

As observed from Table 1 and Table 2, the identified anomalous blocks (e.g., ROI-96, exhibiting the largest ΔLST and ΔSTD) on average, demonstrate higher ΔLST and ΔSTD values compared to blocks with the lowest anomaly scores. For instance, Block ROI-96, which recorded the highest ΔLST and ΔSTD among the anomalous blocks, experienced more than 9°C change in LST and over 13°C change in STD over the decade. In contrast, in blocks with the lowest anomaly scores, the maximum ΔLST was approximately 4.31°C, and ΔSTD was about 6.10°C. This striking disparity in the range of variations underscores that the RX method has successfully distinguished blocks that have undergone significant and persistent thermal changes from other areas. These findings establish a significant link between high anomaly scores and actual thermal fluctuations within the urban environment.

4.2 Visual Validation

To further validate the findings and gain a deeper understanding of the relationship between thermal anomalies and physical changes on the Earth's surface, two blocks were selected from the 22 anomalous zones for more detailed analysis. These blocks serve as illustrative examples of two distinct types of land use change resulting from urban development. First, Figure 4 presents the temperature variation trends for these two selected blocks.

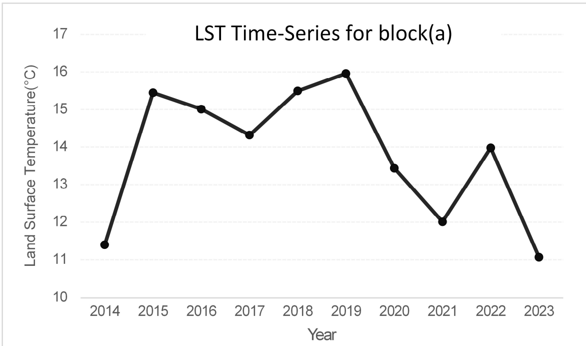

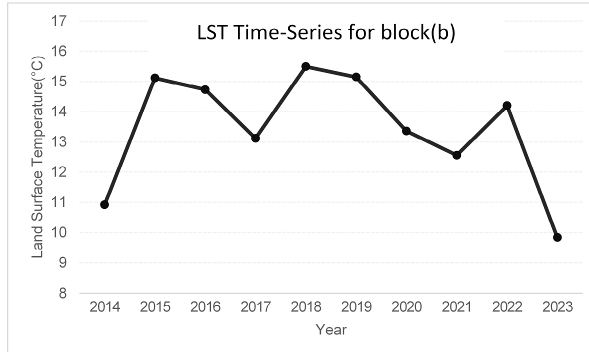

Figure 4 shows the changes in Land Surface Temperature (LST) over the study period (2014–2023) for the selected blocks.

Alongside the identification of significant anomalies, the time series data also reveals certain challenges. For instance, abrupt temperature spikes observed in 2014, which do not necessarily correspond to visible physical changes in the environment may be attributed to sensor noise or specific atmospheric conditions. This issue will be further addressed in the recommendations section. Following the presentation of temperature trends, high-resolution satellite images of the same two blocks from the years 2014 and 2023 are shown in Figure 5.

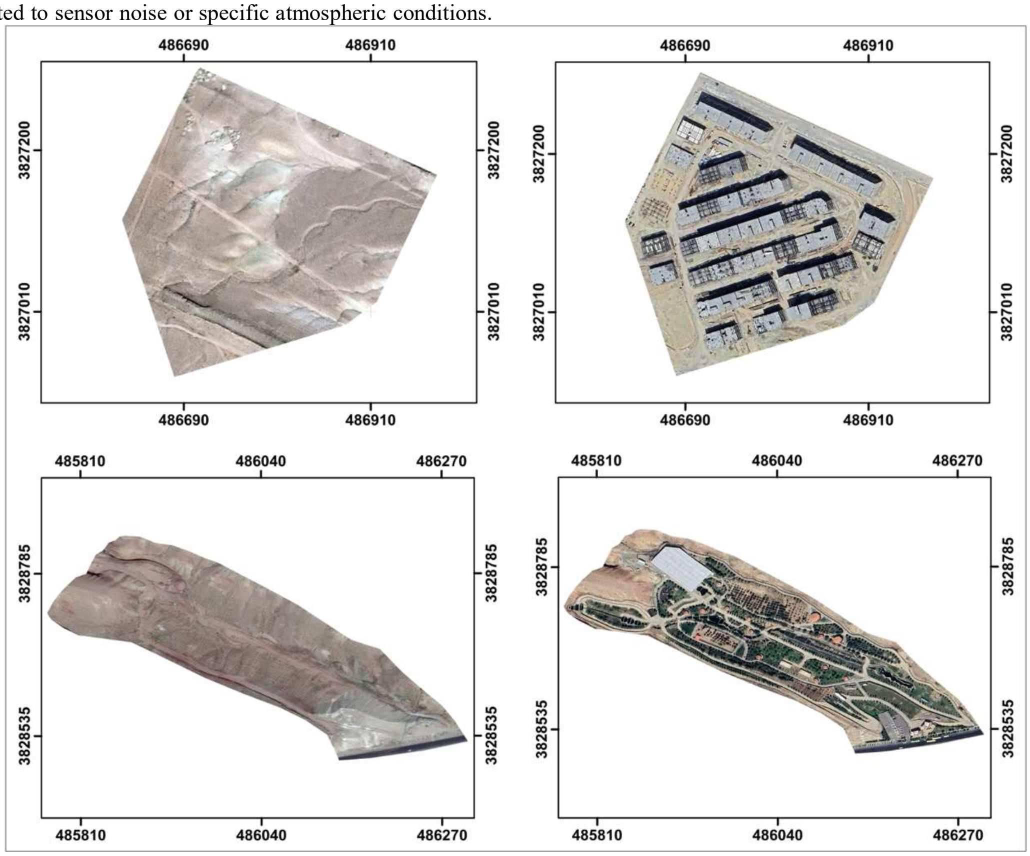

Figure 5. Visual representation of land use changes in the two selected blocks (block(a) and block(b)), whose temperature trends are shown in Figure 4. The figure includes four high-resolution satellite images from Google Earth: images from 2014 are shown in the left column, and those from 2023 appear in the right column. The top row corresponds to block(a), and the bottom row to block(b).

Block(a), which was largely barren land in 2014, had changed into a residential site by 2023. The satellite images from 2023 reveal dirt roads surrounding the area, along with visible concrete and steel columns that suggest ongoing construction and the absence of final infrastructure elements like asphalt. Based on visual interpretation of HRSI, construction activities in this area appear to have begun around 2018. In general, urban development and the replacement of natural surfaces with impervious materials such as concrete and asphalt are expected to lead to increased land surface temperatures (LST) due to higher heat absorption, increasing surface emissivity, reduced evapotranspiration, and overall disruption of natural cooling mechanisms (Kalhor et al., 2024; Luo and Wu, 2021).

However, as shown in the LST trend for block(a) in Figure 4, the expected continuous temperature rise is not observed. Instead, there's a noticeable decline in surface temperature leading up to 2023 an outcome that runs counter to conventional expectations. One possible explanation is the “under-construction” nature of the site. At this phase, disturbed soils and exposed construction materials may behave thermally different from either fully paved surfaces or untouched barren land (Ponomareva et al., 2021). This intermediate state may result in altered heat capacity, or even allow for moisture evaporation following rainfall events, potentially dampening the typical temperature rise observed in more developed urban zones (Azad et al., 2022).

Block(b), in contrast, was also barren in 2014 but had been converted into a green space by 2023, featuring landscaped gardens, a small artificial lake, and shaded structures resembling a well-developed urban park. Such a transition from bare soil to vegetated cover is typically associated with significant reductions in LST. Vegetation helps cool the surface through evapotranspiration and shading, both of which contribute to lowering ambient and surface temperatures (Ghale et al., 2025). The LST trend for this block, as shown in Figure 4, clearly demonstrates a consistent and notable decrease, which aligns well with the observed land use change.

The selection of these two blocks as case studies is especially meaningful, as they represent two contrasting yet common forms of urban land transformation: construction-driven development and the creation of green spaces. This visual validation using high-resolution satellite imagery not only supports our findings regarding thermal anomaly detection in the study area, but also highlights the tangible relationship between LST variations and physical changes on the ground. In both cases, there was a reasonably strong correspondence between the identified anomalous zones and the visible transformations observed in the images, although in more complex situations, such as that of block(a), a more nuanced analysis is required to fully understand the thermal behavior across different stages of urban development.

5. Conclusion

The approach focused on identifying and diagnosing thermal anomalies in Qom's urban blocks using time-series analysis of Landsat 8 TIR imagery. By combining MAD preprocessing and the RX anomaly detection algorithm, the method successfully identified 22 blocks exhibiting significant thermal changes from 2014 to 2023.

This study demonstrated that the proposed approach based on winter LST and STD time-series analysis using MAD filtering and the RX anomaly detector can effectively identify urban blocks undergoing meaningful land-use changes. Quantitative results showed that the selected blocks exhibited the most significant temperature variations. Furthermore, qualitative validation confirmed a strong correspondence between thermal anomalies and real-world urban transformations in Qom.

Quantitative results highlighted that these anomalous blocks underwent substantial shifts in both LST (up to 9.07°C) and STD (up to 13.21°C), in stark contrast to non-anomalous blocks. These findings underscore the method’s ability to distinguish blocks with fundamental land-use changes from those with natural thermal fluctuations.

The qualitative validation using high-resolution imagery (Figure 5) confirmed that many anomalies corresponded to observable changes such as bare earth to buildings or barren areas to gardens. These results suggest that LST and STD time-series analysis is a practical tool for urban change monitoring and identification of areas prone to development or environmental transformation.

6. Recommendations for Future Work

While our approach proved effective, this study faced certain limitations that pave the way for future enhancements. We observed that abrupt temperature shifts in some years (e.g., 2014) did not always correspond to actual on-the-ground changes, likely reflecting residual sensor noise or atmospheric anomalies.

To build upon these findings, future research could significantly improve accuracy and reliability. We recommend incorporating more advanced filtering techniques to better distinguish true signals from noise. Furthermore, integrating complementary data sources, such as the rich detail from hyperspectral bands, would offer deeper insights into surface material changes. Finally, conducting comprehensive field validation remains essential to conclusively link thermal data with real-world transformations and strengthen the model’s credibility.

7. References

Azad, M., Mokhtarzade, M., Safdarinezhad, A., Siami, A., 2022. Relative Surface Heat Capacity Mapping using the Day and Night Time Series of MODIS Images and Digital Elevation Models (Case study: Semnan Deserts, Iran). J. RS GIS Nat. Resour. 15, 95–118. https://doi.org/10.30495/GIRS.2022.697077

Dutta, K., Basu, D., Agrawal, S., 2018. TEMPORAL AND SPATIAL ANALYSIS OF URBAN HEAT ISLAND USING LANDSAT SATELLITE DATA: TWO INDIAN CASE STUDIES. ISPRS Ann. Photogramm. Remote Sens. Spat. Inf. Sci. IV–5, 71–78. https://doi.org/10.5194/isprs-annals-IV-5-71-2018

Edan, M., Maarouf, R., Hassan, J., 2021. Predicting the impacts of land use/land cover change on land surface temperature using remote sensing approach in Al Kut, Iraq. Phys. Chem. Earth Parts ABC 123, 103012. https://doi.org/10.1016/j.pce.2021.103012

Effat, H., Hassan, O., 2014. Change detection of urban heat islands and some related parameters using multi-temporal Landsat images; a case study for Cairo city, Egypt. Urban Clim. 10. https://doi.org/10.1016/j.uclim.2014.10.011

Evgrafova, A., Vetrov, A., Vladislav, S., Frick, P., 2024. Impact of urban morphology on land surface temperature. Res. Sq. https://doi.org/10.21203/rs.3.rs-3939661/v1

Fakhri, A., Sayadi, S., Naghavi, H., Latifi, H., 2022. A novel vegetation index-based workflow for semi-arid, sparse woody cover mapping. J. Arid Environ. 201, 104748. https://doi.org/10.1016/j.jaridenv.2022.104748

Ghale, B., Mamgain, S., Gupta, K., Roy, A., 2025. Urban Parks and their Cooling Potential: Evaluating how Park Characteristics Affects Land Surface Temperature. Int. Arch. Photogramm.

Remote Sens. Spat. Inf. Sci. XLVIII-M-5–2024, 29–35. https://doi.org/10.5194/isprs-archives-XLVIII-M-5-2024-29-2025

Huang, X., Wang, Y., 2019. Investigating the effects of 3D urban morphology on the surface urban heat island effect in urban functional zones by using high-resolution remote sensing data: A case study of Wuhan, Central China. ISPRS J. Photogramm. Remote Sens. 152, 119–131. https://doi.org/10.1016/j.isprsjprs.2019.04.010

Kachar, H., Vafsian, A.R., Modiri, M., Enayati, H., Safdari Nezhad, A.R., 2015. EVALUATION OF SPATIAL AND TEMPORAL DISTRIBUTION CHANGES OF LST USING LANDSAT IMAGES (CASE STUDY:TEHRAN). Int. Arch. Photogramm. Remote Sens. Spat. Inf. Sci. XL-1/W5, 351–356. https://doi.org/10.5194/isprsarchives-XL-1-W5-351-2015

Kalhor, R., Safdarinezhad, A., Behnabian, B., 2024. Persistent heat islands monitoring of Tehran metropolis using temporal analysis of Landsat-8 satellite images. Environ. Sci. Pollut. Res. 31, 58541–58561. https://doi.org/10.1007/s11356-024-35022-x

Luo, H., Wu, J., 2021. Effects of urban growth on the land surface temperature: a case study in Taiyuan, China. Environ. Dev. Sustain. 23, 1–27. https://doi.org/10.1007/s10668-020-01087-0

Mansourmoghaddam, M., Rousta, I., Ghafarian Malamiri, H., Sadeghnejad, M., Krzyszczak, J., Ferreira, C.S.S., 2024. Modeling and Estimating the Land Surface Temperature (LST) Using Remote Sensing and Machine Learning (Case Study: Yazd, Iran). Remote Sens. 16. https://doi.org/10.3390/rs16030454

Ponomareva, T.V., Litvintsev, K.Yu., Finnikov, K.A., Yakimov, N.D., Sentyabov, A.V., Ponomarev, E.I., 2021. Soil Temperature in Disturbed Ecosystems of Central Siberia: Remote Sensing Data and Numerical Simulation. Forests 12. https://doi.org/10.3390/f12080994

Salih, M., Jasim, O., Hassoon, K., Abdalkadhum, A., 2018. Land Surface Temperature Retrieval from LANDSAT-8 Thermal Infrared Sensor Data and Validation with Infrared Thermometer Camera. Int. J. Eng. Technol. 7, 608. https://doi.org/10.14419/ijet.v7i4.20.27402

Ullah, N., Siddique, M.A., Ding, M., Grigoryan, S., Khan, I.A., Kang, Z., Tsou, S., Zhang, T., Hu, Y., Zhang, Y., 2023. The Impact of Urbanization on Urban Heat Island: Predictive Approach Using Google Earth Engine and CA-Markov Modelling (2005-2050) of Tianjin City, China. Int. J. Environ. Res. Public. Health 20. https://doi.org/10.3390/ijerph20032642

Xian, G., Shi, H., Mueller, C., Hussain, R., Sayler, K., Howard, D., 2023. Monitoring Long-Term Changes of Urban Surface Temperature Using Time-Series Land Cover and Remote Sensing Data Across 50 Major Cities in the United States, in: IGARSS 2023 - 2023 IEEE International Geoscience and Remote Sensing Symposium. pp. 321–324. https://doi.org/10.1109/IGARSS52108.2023.10282543

Zhang, W., Wang, Z., Pinsky, E., 2025. Mean Absolute Deviation for Hyperexponential and Hypoexponential Distributions. Oper. Res. Appl. Int. J. 12, 19–37. https://doi.org/10.5121/oraj.2025.12202

Zhao, C., Yao, X., Huang, B., 2016. Real-Time Anomaly Detection Based on a Fast Recursive Kernel RX Algorithm. Remote Sens. 8, 1011. https://doi.org/10.3390/rs8121011